Constitutive activation of Stat3 signaling abrogates apoptosis in squamous cell carcinogenesis *in vivo*

Jennifer Rubin Grandis*†‡, Stephanie D. Drenning*, Qing Zeng*, Simon C. Watkins§, Mona F. Melhem¶, Sohei Endo*, Daniel E. Johnson†‖, Leaf Huang†, Yukai He†, and Jae D. Kim*

Departments of *Otolaryngology, ¶Pathology, §Cell Biology and Physiology, ‖Medicine, and †Pharmacology, University of Pittsburgh School of Medicine and University of Pittsburgh Cancer Institute, Pittsburgh, PA 15213

Communicated by James E. Darnell, Jr., The Rockefeller University, New York, NY, December 27, 1999 (received for review November 4, 1999)

Field cancerization predisposes the upper aerodigestive tract mucosa to the formation of multiple primary tumors, when exposed to environmental carcinogens. Up-regulation of epidermal growth factor receptor occurs early in squamous cell carcinogenesis and is critical for the loss of growth control in a variety of human cancers, including head and neck squamous cell carcinomas. In these tumor cells in culture, epidermal growth factor receptor stimulation initiates signaling via persistent activation of selective STAT proteins. To determine the timing of Stat3 activation in head and neck carcinogenesis, we studied the expression and constitutive activation of Stat3 in tumors and normal mucosa from patients with head and neck cancer compared with mucosa from controls without cancer. Stat3 was up-regulated and constitutively activated in both primary human head and neck tumors as well as in normal mucosa from these cancer patients compared with control normal mucosa from patients without cancer. *In vivo* liposome-mediated gene therapy with a Stat3 antisense plasmid efficiently inhibited Stat3 activation, increased tumor cell apoptosis, and decreased Bcl-x_L expression in a head and neck xenograft model. These findings provide evidence that constitutively activated Stat3 is an early event in head and neck carcinogenesis that contributes to the loss of growth control by an anti-apoptotic mechanism.

Squamous cell carcinoma of the head and neck (SCCHN) is an epithelial malignancy affecting the mucosa of the upper aerodigestive tract. ''Field cancerization'' was originally proposed to describe the diffuse effects on the tissues as a result of exposure to environmental carcinogens such as tobacco and alcohol (1). A generalized mucosal diathesis is supported in SCCHN by the high incidence of second primary tumors of the upper aerodigestive tract that characterizes these patients (2). If patients are cured of their primary SCCHN, they will most likely die of a second aerodigestive tract cancer. SCCHN patients who develop a second cancer have only a 25% 5-year survival rate (3). The critical signaling pathways that regulate SCCHN proliferation and/or apoptosis are incompletely understood.

Overexpression of type α transforming growth factor (TGF-α) and its receptor, the epidermal growth factor receptor (EGFR), have been demonstrated in transformed squamous epithelium and premalignant dysplasias as well as in normal mucosa from cancer patients compared with levels in normal mucosa from patients without cancer, suggesting that activation of TGF-α/EGFR autocrine growth is an early event in head and neck tumorigenesis (4–6). This increased expression of TGF-α and EGFR mRNA and protein is primarily caused by activated gene transcription (as opposed to increased gene copy number or prolonged mRNA half life) (7). It is well established that TGF-α derived from either autocrine or paracrine sources plays an essential role in the malignant transformation and progression of SCCHN by regulating the growth and survival of head and neck tumor cells (8–10). TGF-α induces intracellular signaling through stimulation of EGFR, which contains a cytoplasmic domain with intrinsic protein tyrosine kinase activity. In response to ligand, EGFRs dimerize and become phosphorylated on multiple tyrosine residues. These phosphotyrosines, in turn, allow the activated receptor to recruit STATs (signal transducers and activators of transcription) to tyrosines Y1068 and Y1086 (11). Direct interaction between STAT protein src-homology 2 domains and the activated receptor leads to STAT phosphorylation followed by dimerization and translocation to the nucleus. In the nucleus, STATs bind to DNA-response elements in promoters, thus regulating growth factor/cytokine-directed gene expression (12–17).

To date, seven STATs have been identified: STAT1, -2, -3, -4, -5A, -5B, and -6. Stat5A and Stat5B are encoded by distinct genes whereas STAT1 and STAT3 exhibit two isoforms each, resulting from alternative splicing (Stat1 α/β and Stat3 α/β). An emerging literature suggests that STAT signaling may play a critical role in cancer formation and progression [for review, see the work by Garcia and Jove (18)]. There is constitutively elevated tyrosine phosphorylation and DNA-binding activity of Stat3 in fibroblasts stably transformed by the Src oncoprotein (19). Further investigation demonstrated that Stat3 activation is required for Src-mediated oncogenesis in which transformation by v-Src leads to Stat3-specific gene expression (20–21). Increased activation of Stat3 has been observed in a variety of human malignancies, including breast cancers and breast cancer-derived cell lines compared with benign lesions and normal breast epithelium (22–24). In multiple myeloma patients, constitutive Stat3 activation is detected in bone marrow mononuclear cells as well as an IL-6-dependent human myeloma cell line in which Stat3 signaling results in resistance to apoptosis and up-regulation of the anti-apoptotic protein, Bcl-x_L (25).

We previously reported that TGF-α/EGFR autocrine signaling is activated early in SCCHN carcinogenesis (1, 2). Further investigation in our laboratory demonstrated that both TGF-α production and EGFR expression by SCCHN cells are linked to constitutive Stat3 activation *in vitro*. Using antisense oligonucleotides or dominant negative mutants of Stat3, we demonstrated growth inhibition of SCCHN cells (26). The expression and activation of STAT proteins in premalignant lesions and corresponding human carcinomas has not been studied previously. To elucidate the role of Stat3 activation in head and neck cancer progression, we measured Stat3 expression/activation levels in tissues from SCCHN patients compared with mucosa from controls without cancer. Further investigation using an antisense gene therapy approach was undertaken to determine the biologic consequences of Stat3 down-modulation *in vivo*. These results indicate that constitutive Stat3 activation early in head and neck carcinogenesis may enhance tumor progression by blocking tumor cell apoptosis.

Abbreviations: EGFR, epidermal growth factor receptor; SCCHN, squamous cell carcinoma of the head and neck; TGF-α, type α transforming growth factor; EMSA, electrophoretic mobility shift assay; hSIE, high-affinity serum inducible element; SIF, sis-inducible factor.

‡To whom reprint requests should be addressed at: The Eye and Ear Institute, Suite 500, 200 Lothrop Street, Pittsburgh, PA 15213. E-mail: jgrandis+@pitt.edu.

The publication costs of this article were defrayed in part by page charge payment. This article must therefore be hereby marked "*advertisement*" in accordance with 18 U.S.C. §1734 solely to indicate this fact.

Table 1. Clinicopathologic characteristics of 19 head and neck cancer patients evaluated prospectively for Stat3 activation/expression

Gender	
Male	15 (79%)
Female	4 (21%)
Age	Mean, 60.83 years; Median, 62.5 years; range, 38–76 years
Tumor Site	
Oral cavity	8 (42%)
Oropharynx	4 (21%)
Hypopharynx	2 (10%)
Larynx	4 (21%)
Unknown	1 (5%)
T Stage	
1–2	12 (63%)
3–4	7 (37%)
N Stage	
0–1	11 (58%)
2	8 (42%)
Tumor differentiation	
Well	1 (5%)
Moderate	16 (90%)
Poor	1 (5%)

Methods

Patients and Tissue Samples. Samples of squamous cell carcinoma and normal mucosa distant from the tumor (generally, several centimeters away) were obtained from 19 patients undergoing primary surgical resection for head and neck cancer at the University of Pittsburgh Medical Center from January, 1997 to June, 1998 (Table 1). Samples of normal oropharyngeal mucosa were obtained from seven gender- and age-matched (±5 years) control patients without cancer undergoing non-oncological surgical procedures, such as uvulopalatopharyngoplasty for obstructive sleep apnea syndrome.

Immunoblotting. Whole-cell extracts from patient tissues were mixed with 2× SDS sample buffer (125 mmol/liter Tris·HCl, pH 6.8/4% SDS/20% glycerol/10% 2-mercaptoethanol) at 1:1 ratio and were heated for 5 min at 100°C. Proteins (50 μg/lane) were separated by 12.5% SDS/PAGE and were transferred onto a nitrocellulose membrane (Micron Separations, Westboro, MA). Prestained molecular weight markers (GIBCO) were included in each gel. Membranes were blocked for 30 min in Tris-buffered saline (TBS) (10 mmol/liter Tris·HCl, pH 7.5/150 mmol/liter NaCl) with 0.5% Tween-20 (TBST) and 5% BSA. After blocking, membranes were incubated for 60 min with a Stat3 phosphotyrosine-specific polyclonal Ab (Chemicon), a Bcl-x_L mouse anti-human monoclonal antibody (Santa Cruz Biotechnology), or a Bax rabbit polyclonal antibody (Santa Cruz Biotechnology) in TBST and 1% BSA. After washing the membranes three times with TBST (5 min each), they were incubated with horseradish peroxidase-conjugated secondary antibody in TBST and 1% BSA for 30 min. Subsequently, membranes were washed three times with TBST and were developed by using the enhanced chemiluminescence (ECL) detection system (Amersham). Quantitation of the signal for Stat3 or phosphorylated Stat3 was performed by using a Molecular Dynamics Personal Densitometer SI and IMAGEQUANT software (Image Products International, Chantilly, VA). Normalization between blots was accomplished by running aliquots of U937 cell lysates (40 μg), a human myeloid leukemia cell line that overexpresses Stat3, on each gel.

Immunohistochemistry. Five-micrometer sections of human tissues, previously snap-frozen in liquid nitrogen, were cut and fixed in cold acetone for 1 min. Slides were stained with a polyclonical rabbit anti-mouse phospho-Stat3 (Tyr705) antibody (New England Biolabs), using a 3% hydrogen peroxide/methanol solution as a blocking agent. Slides were incubated at 4°C overnight by using a 1:100 dilution of the primary antibody, then were developed with the LSAB2 kit (Dako).

Electrophoretic Mobility Shift Assay (EMSA). Whole cell extracts were prepared and EMSAs performed on 4% native polyacrylamide gels as described (27, 28). Stat3 activation was evaluated by using binding reactions with 20 μg of extracted protein, and radiolabeled high-affinity serum inducible element (hSIE) duplex oligonucleotide was used to clone and characterize Stat3 (29). Quantitation of the Stat3 signal was performed by scanning the SIF-A band using a Molecular Dynamics Personal Densitometer SI and IMAGEQUANT software. Normalization between blots was accomplished by running aliquots of U937 cell lysates (5 μg) that demonstrate activation of Stat3 on each gel. Activation of Stat1 and Stat3 may be assessed by determining the presence of DNA-binding activity as manifested by sis-inducible factor (SIF) activity. This is resolved into three different protein-DNA complexes termed SIF-A (representing Stat3 homodimer), SIF-B (representing Stat1/Stat3 heterodimer), and SIF-C (representing Stat1 homodimer). For supershift experiments, extracts were preincubated with Stat1 polyclonal antibody (C-24; Santa Cruz Biotechnology) or Stat3 polyclonal antibody (C-20, Santa Cruz Biotechnology).

***In Situ* hSIE Binding Assay.** For standard light microscopy of cryostat sections, tissues were lightly fixed in 2% paraformaldehyde, were infused with 30% sucrose overnight, and were frozen in liquid nitrogen-cooled isopentane. Five-micrometer sections were cut on a Microm cryostat, were mounted on polylysine-coated or Superfrost (Fisher) slides, and were labeled. The samples were prepared for hybridization by three 5-min washes in 1× PBS followed by incubation in a solution of 1× PBS containing 0.1 mg/ml of DNase Rq1. Thereafter, the samples were postfixed in a 1× PBS solution containing 20% paraformaldehyde for 30 min at room temperature followed by three 5-min 1× PBS washes. ^{35}S-labeled hSIE duplex oligonucleotide (via end-labeling) was then applied to the samples by placing ≈100 μl of probe onto 25 × 25 mm coverslips and rolling the slides onto the coverslips. The slides were placed into a microscope box containing a moist paper towel and were allowed to incubate for 60 min at 30°C. After hybridization, the samples were washed 3 times in 1× PBS and were subjected to an ethanol dehydration series. After complete drying, the slides were dipped into Kodak NTB-2 (Eastman Kodak) autoradiography emulsion. The dipped slides were air-dried for 4 h, were placed in a light-tight container, and were stored in a 4°C refrigerator for 7 days. At the end of the 7 days, the samples were developed by using D-19 developer for 4 min and Rapid Fix photographic fixer for 4.5 min. The samples were counterstained with toluidine blue and then were coverslipped by using cytoseal mounting media.

Plasmid Construct and Cloning. We modified the original U6 expression plasmid (pGEMmU6, from S. Noonberg, University of California at San Francisco Cancer Research Institute) as described (30). A 51-nt sense sequence and a 215-nt antisense oligonucleotide sequence corresponding to the translation start site of the human Stat3 cDNA were synthesized and cloned into the modified U6 construct to generate two new plasmids, U6-Stat3-S and U6-Stat3-AS, which were verified by sequence analysis.

***In Vivo* Tumor Xenograft Studies.** The cell line, 1483, is a well described SCCHN cell line derived from a tumor of the retromolar trigone region of the oropharynx (31) and was kindly provided by R. Lotan (University of Texas M. D. Anderson Cancer Center, Houston, TX). Female athymic nude mice nu/nu (4–6 weeks old; 20 ± 2 g; Harlan–Sprague–Dawley) were implanted with 1 × 10^6

cells into the right flank with a 26-gauge needle/1 ml tuberculin syringe. Approximately 14–21 days later, when the tumor nodules were established (≈2 × 2 mm in diameter), mice were randomly assigned to treatment groups (liposomes alone, Stat3 sense construct plus liposomes, or Stat3 antisense construct plus liposomes). There were 10 mice in each treatment group. Intratumoral injection of plasmid DNA (50 μg) complexed with DC-Chol liposomes (50 nmol) in a volume of 50 μl was delivered. Mice were killed 2 days after a single injection, and tumors were harvested for analysis. Experiments were repeated twice to ensure reproducibility. Animal care was in strict compliance with institutional guidelines established by the University of Pittsburgh, the Guide for the Care and Use of Laboratory Animals [National Academy of Sciences (1996)], and the Association for Assessment and Accreditation of Laboratory Animal Care International.

***In Vivo* Apoptosis Determinations/DNA Fragmentation.** The percentage of apoptotic cells in tumors treated with the Stat3 antisense (versus sense) construct was determined by staining for DNA fragmentation (ApopTag). Tumors were harvested, sectioned, fixed in formalin, and paraffin-embedded, then were incubated with proteinase K diluted in PBS for 20 min and washed four times in water. Slides were then incubated in 3% H_2O_2 in PBS for 5 min and were washed twice in PBS. Each section was incubated with a terminal transferase enzyme that catalyzes the addition of digoxigenin-labeled nucleotides to the 3′-OH ends of the fragmented DNA for 15 min at 37°C. Slides were then placed in stop buffer for 30 min at 37°C, followed by washing three times in PBS for 5 min. Negative controls were obtained by substituting dH_2O for the terminal deoxynucleotidyl transferase mix. Slides were read and scored under 400× magnifications for the number of positive cells per five high power fields by using computerized image analysis (SAMBA 4000 Image Analysis System, Image Products International).

Statistics. Statistical analyses were performed by using STATVIEW 4.5J software (Abacus Concepts, Berkeley, CA). For the patient samples, ANOVA was used to analyze all three groups. Specifically, tumors were compared with normal mucosa samples from SCCHN patients (paired), and normal mucosa from SCCHN patients was compared with control normal mucosa from patients without cancer. For animal experiments, comparisons were restricted to mice treated in the same experiment. For apoptosis studies, the statistical significance of differences in the number of apoptotic cells was assessed by use of Student's *t* test (two-sided) that assured unequal variance.

Results

Stat3 Activation/Expression in SCCHN Tissues. The concept of "field cancerization" or "condemned mucosa," whereby multiple foci of premalignant changes occur in the surrounding histologically normal mucosa adjacent to the tumor as a result of the exposure of the entire epithelium to carcinogenic agents (e.g., tobacco and alcohol), has been postulated to explain the susceptibility of patients with SCCHN to the high incidence of synchronous and metachronous tumors (1, 32). EMSAs were performed to determine the level of constitutive activation of Stat3 in the tumor and histologically normal mucosa samples from SCCHN patients. Repeated EMSA analysis on a subset of samples was performed, and the variability ranged from 3 to 7%. Activation of Stat3 protein was found to be 10.6-fold higher in tumors and 8.8-fold higher in normal mucosa from cancer patients compared with normal mucosa from non-cancer patients ($P = 0.012$ and $P = 0.018$, respectively) (Fig. 1 *A* and *B*; data not shown). The predominant complexes formed were SIF-A (Stat3 homodimers) and SIF-B (Stat3 and Stat1 heterodimers). The SIF-C (Stat1 homodimers) complex was either undetectable or present at very low levels. To verify that the constitutive SIF-A and SIF-B complexes contained Stat3 and Stat1, we performed supershift analysis by using appropriate antisera (Fig. 1*C*).

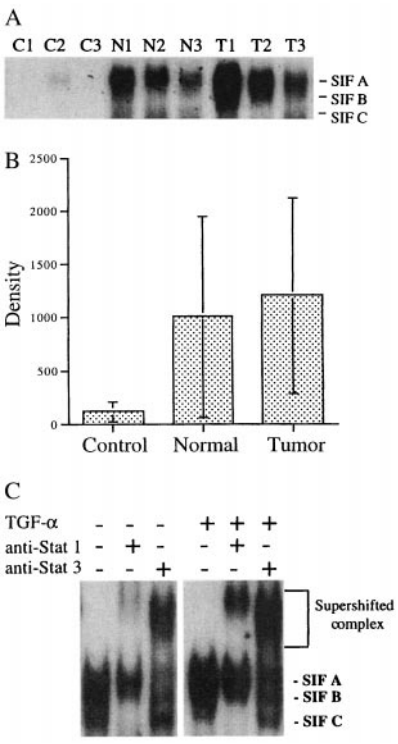

Fig. 1. Constitutive Stat3 activation in normal mucosa and tumors from SCCHN patients. (*A*) Extracts (20 μg) were prepared from representative tumors (T1–3) and normal mucosa samples (N1–3) from SCCHN patients as well as normal mucosa biopsies from patients without cancer (C1–3). EMSA was performed with radiolabeled hSIE duplex oligonucleotide. The positions of the SIF-A complex (Stat3 homodimer), SIF-B complex (Stat1/Stat3 heterodimer), and SIF-C complex (Stat1 homodimer) are indicated on the right. (*B*) cumulative results of Stat3 activation levels in control and SCCHN tissues showing increased constitutive Stat3 activation levels (SIF-A signal) in tumors ($P = 0.012$) and normal mucosa from SCCHN patients ($P = 0.018$) compared with normal mucosa from control patients without cancer. (*C*) EMSA was performed by using extracts of a representative SCCHN tumor before and after stimulation with TGF-α (30 ng/ml for 30 min). Extracts were preincubated with rabbit antibody to Stat1 (C-24) or Stat3 (C-20) or no antibody, as indicated. The position of the SIF-A, -B, and -BC complexes and the supershifted complexes are indicated on the right.

A potential pitfall of EMSA analysis using tissue samples is the contribution of "contaminating" cells (e.g., stromal cells and inflammatory cells) to the level of Stat3 protein activation detected. To localize the activated Stat3 in tissue sections, [^{35}S]methionine was used to metabolically label the Stat3 DNA binding oligonucleotide duplex (hSIE) as described (33). An oligonucleotide probe for NF-κB was used to control for the specificity of labeling. As demonstrated in Fig. 2, SCCHN tumors demonstrated elevated levels of activated Stat3 compared with normal epithelium from controls that was primarily concentrated at the tumor/stromal interface. High power microscopy demonstrated that the cells containing activated Stat3 were epithelial cells and not tumor-infiltrating lymphocytes.

Increased Stat3 activation can occur through several potential mechanisms, including elevated constitutive levels of Stat3 protein and increased Stat3 tyrosine phosphorylation. Normal mucosa samples from both cancer patients and controls were used as comparison groups to determine the potential timing of alterations in Stat3 expression during SCCHN carcinogenesis. To determine whether the increase in constitutive Stat3 activation was associated with increased protein expression, we performed immunoblotting studies using antisera to Stat3. These

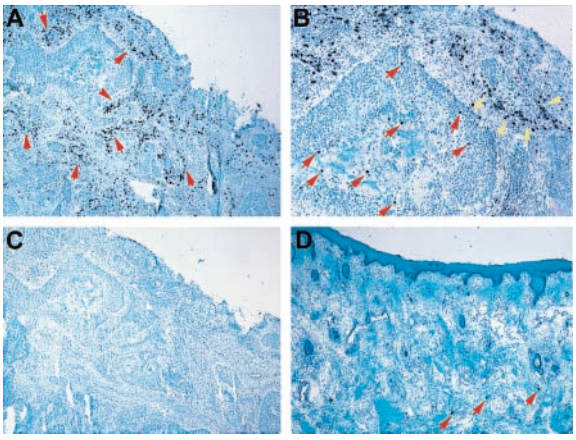

Fig. 2. Localization of activated Stat3 to tumor cells using an *in situ* hSIE binding assay. (*A*) At low power (50× magnification), a large number of positive cells are seen localized to tumor cells (red arrows). (*B*) When observed under high power (100× magnification), the positive cells are closely associated with the periphery of the tumor parenchyma (yellow arrows) and often penetrate into the parenchyma itself (red arrows). (*C*) Tumor sections labeled with a ^{35}S-labeled oligonucleotide probe specific to NF-κB show no positive cells, indicating that the ^{35}S-hSIE labeling is specific. (*D*) Normal mucosa from a control without cancer labeled with hSIE probe shows a limited number of positive cells (red arrows).

experiments demonstrated a 2.19-fold increase in Stat3 protein in SCCHN tumors compared with normal mucosa from noncancer patients ($P = 0.021$) and a 2.32-fold increase in tumors compared with normal mucosa from SCCHN patients ($P = 0.006$) (data not shown). Immunohistochemistry confirmed that the epithelial cells of the tissue samples were the primary source of Stat3 protein expression (data not shown). Phosphotyrosine immunoblotting was performed to determine whether the increased Stat3 activity detected on EMSA was associated with elevated tyrosine phosphorylation. These results demonstrated increased phosphorylated Stat3 in both tumors ($P = 0.002$) and normal mucosa samples from SCCHN patients ($P < 0.001$) compared with normal mucosa from control patients (Fig. 3*A*).

To investigate the expression of activated Stat3 in the condemned mucosa from SCCHN patients, we stained representative tissues with a phosphospecific Stat3 antibody. Immunohistochemistry demonstrated that phosphorylated Stat3 was restricted to the basal epithelial cells in normal mucosa from patients without cancer. In contrast, phosphorylated Stat3 was present throughout the epithelium in normal mucosa from cancer patients and was overexpressed in tumors (Fig. 3 *B–D*). The detection of increased Stat3 activation and elevated Stat3 tyrosine phosphorylation in the condemned mucosa of SCCHN patients suggests that up-regulation of Stat3 activity represents a relatively early alteration in SCCHN carcinogenesis, followed by up-regulation of Stat3 protein expression.

Stat3 Activation Is Linked to TGF-/EGFR Signaling *in Vivo*. To verify that the constitutive Stat3 activation detected in SCCHN tissues was a specific result of EGFR signaling, we analyzed human tumor xenografts treated with an EGFR antisense gene therapy construct that we have previously demonstrated to inhibit EGFR expression and SCCHN tumor growth *in vivo* (30). After intratumoral injection of EGFR antisense DNA (50 μg) complexed with DC-Chol liposomes (50 nmol), tumors were harvested and EMSAs were performed. SCCHN tumors treated with EGFR antisense gene therapy demonstrated decreased constitutive Stat3 activation compared with tumors treated with liposomes alone (data not shown).

Liposome-Mediated Antisense Gene Therapy Blocks Stat3 *in Vivo*. The detection of constitutively increased Stat3 in SCCHN tissues suggests that Stat3 may play a critical role in the progression of head and neck tumors. To determine the consequences of down-modulating Stat3 *in vivo*, we generated a Stat3 antisense gene expression vector for use in a SCCHN xenograft model. Fifty micrograms of plasmid DNA complexed with DC-chol liposomes was injected into each tumor, and mice were killed 48 h later, when tumors were harvested for protein. EMSAs were performed to determine the consequences of Stat3 antisense gene therapy on constitutive Stat3 activity. Fig. 4 *A* and *B* demonstrates decreased constitutive Stat3 activation in the tumors treated with the Stat3 antisense gene (plus liposomes) compared with levels in the tumors treated with the corresponding sense construct (plus liposomes) ($P = 0.001$) or the tumors that received liposomes alone ($P = 0.001$).

Stat3 Antisense Gene Therapy Induces Apoptosis. Previous studies have suggested that activation of Stat3 may abrogate apoptosis in

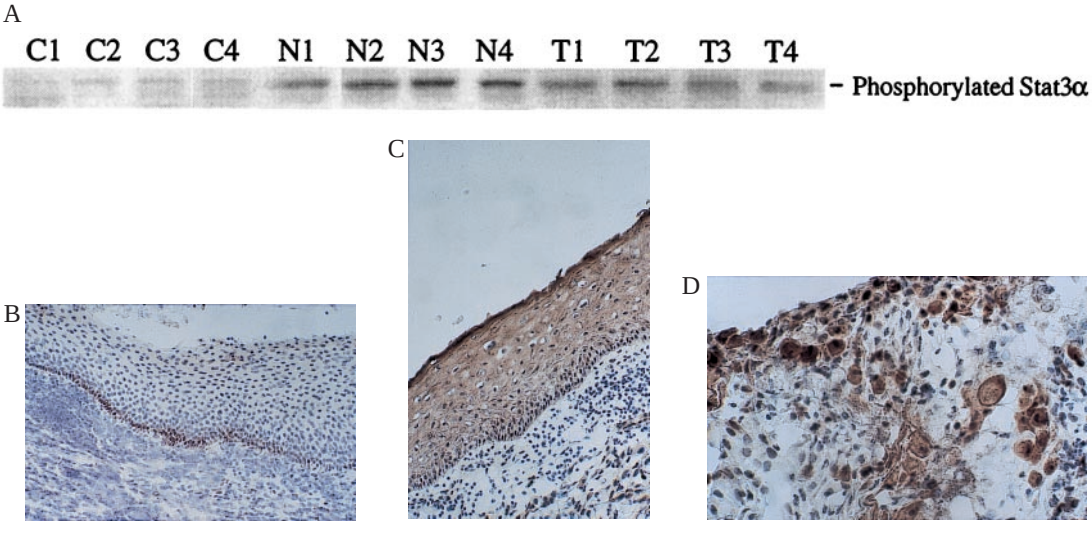

Fig. 3. Stat3 tyrosine phosphorylation. (*A*) Immunoblotting of protein extracts (50 μg) from representative control normal mucosa from patients without cancer (C1–4), normal mucosa from SCCHN patients (N1–4), and SCCHN tumors (T1–4) using a phosphospecific anti-Stat3 p-TYR (705) antibody. The position of the phosphorylated Stat3 protein is indicated on the right. (*B*) Stat3 phosphotyrosine immunostaining showing basal epithelial expression in a representative normal mucosa from a patient without cancer. (*C*) Staining throughout the epithelium in a representative sample of normal mucosa from SCCHN patients. (*D*) Increased expression in a representative SCCHN tumor.

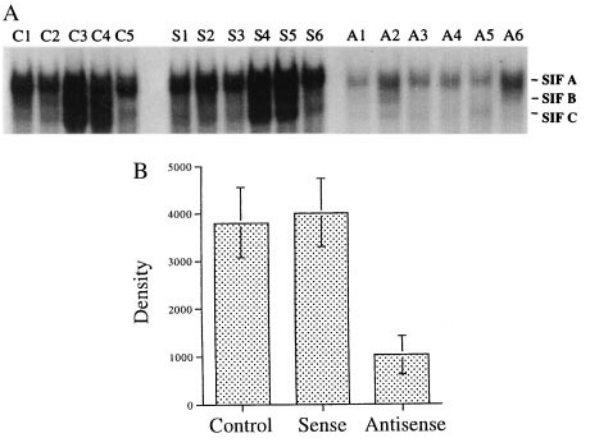

Fig. 4. Decreased Stat3 activation in tumors treated with Stat3 antisense gene therapy. (*A*) EMSA analysis of representative SCCHN xenografts after treatment with Stat3 antisense DNA plus liposomes (A1–6) compared with Stat3 sense DNA plus liposomes (S1–6) or liposomes alone (C1–5). (*B*) Cumulative results demonstrating decreased constitutive Stat3 activation levels (SIF-A band) in SCCHN tumors treated with Stat3 antisense gene therapy compared with the corresponding sense construct plus liposomes ($P = 0.001$) or liposomes alone ($P = 0.001$).

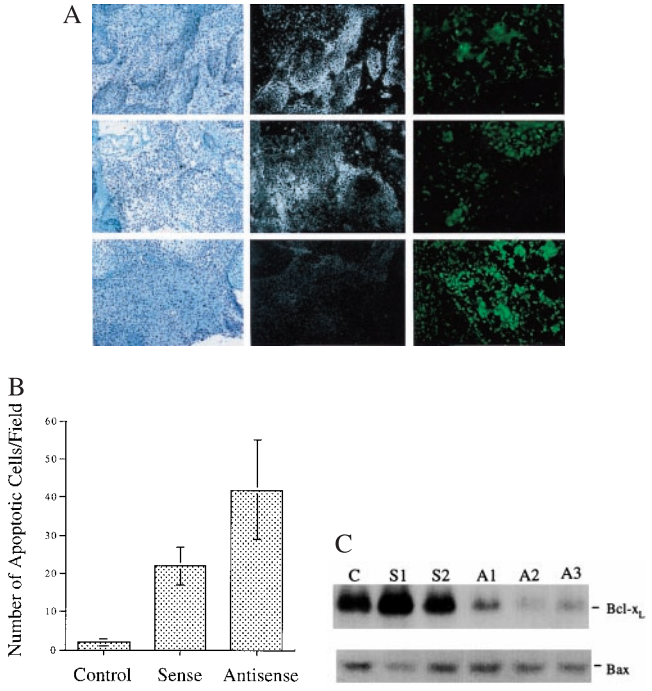

Fig. 5. Stat3 antisense gene therapy *in vivo* is accompanied by decreased hSIE binding and increased apoptosis. (*A*) The column on the left shows *in situ* Stat3 activity in representative SCCHN tumors treated with Stat3 sense DNA plus liposomes, liposomes alone (control), or Stat3 antisense DNA plus liposomes (black dots indicate activated Stat3). The middle column is a darkfield representation of the hSIE activity (white dots indicate activated Stat3). The column on the right shows TUNEL staining of representative SCCHN tumors. (*B*) Cumulative results showing increased apoptosis in SCCHN tumors treated with Stat3 antisense gene therapy compared with Stat3 sense gene therapy ($P = 0.006$) or liposomes alone ($P < 0.001$). (*C*) Bcl-x_L and Bax immunoblotting of representative SCCHN tumors treated with Stat3 antisense DNA plus liposomes (A1–3) compared with Stat3 sense DNA plus liposomes (S1–2) or liposomes alone (*C*).

hematopoietic cells (25, 34). SCCHN cell lines stably transfected with either of two dominant negative Stat3 mutant constructs [3F, where tyrosine 705 in Stat3 is replaced by phenylalanine; 3D, where mutations were inserted at positions important for DNA binding (glutamic acid 434 and glutamic acid 435 were replaced with alanines)] and subjected to serum deprivation for 24 h followed by flow cytometry demonstrated a 4- to 5-fold increase in the number of apoptotic cells (data not shown). To determine whether down-modulation of Stat3 by using Stat3 antisense gene therapy induced apoptosis in human tumors *in vivo*, SCCHN xenografts were harvested from each treatment group when the mice were killed (10 mice/group) and were stained for DNA fragmentation (ApopTag). *In situ* hSIE binding demonstrated decreased Stat3 activity in antisense-treated tumors corresponding to an increase in apoptosis (Fig. 5*A*). Cumulative results demonstrated a 2-fold elevation in the rate of apoptosis in the tumors treated with the Stat3 antisense construct plus liposomes compared with tumors treated with the corresponding sense construct plus liposomes ($P = 0.006$) or liposomes alone ($P < 0.001$); Fig. 5*B*).

Stat3 has been shown to regulate transcription from the bcl-x gene promoter (25). To determine whether Stat3-mediated regulation of apoptosis was associated with modulation of the apoptotic regulatory protein, Bcl-x_L, tumors treated with Stat3 antisense DNA plus liposomes were harvested and analyzed for Bcl-x_L expression using immunoblotting. As demonstrated in Fig. 5*C*, Stat3 antisense gene therapy resulted in decreased Bcl-x_L expression compared with treatment with Stat3 sense DNA plus liposomes or liposomes alone. Immunoblotting of the same extracts using antisera to Bax demonstrated no modulation of these apoptotic regulatory proteins after Stat3 antisense gene therapy (Fig. 5*C*). These results suggest that the apoptotic effects of targeting Stat3 *in vivo* are mediated, in part, by down-modulation of the anti-apoptotic protein, Bcl-x_L.

Discussion

This study provides evidence that both normal mucosa and tumors from head and neck cancer patients, unlike normal squamous epithelium from patients without cancer, demonstrate constitutive overexpression and activation of the EGFR signaling protein, Stat3. Furthermore, targeting Stat3 *in vivo* by using an antisense gene therapy approach induces apoptosis. These results suggest that constitutive activation of Stat3 represents an early event in head and neck carcinogenesis and that EGFR-mediated Stat3 signaling is a critical pathway for tumor progression and apoptotic dysregulation. Several reports indicate that human tumors and tumor-derived cell lines contain constitutively active STAT proteins, most commonly Stat3 (18, 35). Although cytokine or growth factor-dependent activation of STATs is frequently associated with differentiation, constitutive activation is generally characterized by a loss of growth control (36–38).

We have previously demonstrated that head and neck cancers produce TGF-α, which stimulates EGFRs (either on the cell surface or in the cytoplasm) expressed by the cancer cell, thus establishing an autocrine growth pathway (4). The biological importance of this pathway is underscored by our finding that the level of EGFR (or TGF-α) protein expressed in the primary head and neck tumor is a significant predictor of decreased survival, independent of known clinical and pathologic parameters, including regional lymph node metastases (39). Cancer therapies that incorporate EGFR targeting strategies show increasing promise in preliminary reports of phase I clinical trials. Elucidation of the critical downstream EGFR signaling pathways would greatly improve prevention and treatment efforts based on targeting this growth factor receptor. The precise mechanisms by which growth factor-induced cell surface signals are transmitted to the nucleus and ultimately result in cell division are only partially understood. The EGFR contains a cytoplasmic domain with intrinsic protein tyrosine kinase activity. In response to ligand(s), EGFRs dimerize

and become phosphorylated on multiple tyrosine residues. These phosphotyrosines, in turn, allow the activated receptor to associate with other signaling proteins. Several potential EGFR signaling pathways have been described, including Ras/MAP kinase, phosphotidylinositol-3-kinase, phospholipase C, and STATs (40–42). Interaction between many signaling proteins and activated receptor occurs through specific recognition of receptor phosphotyrosine residues by conserved src-homology 2 domains in the cytoplasmic signaling protein. STATs serve the dual function of signal transducers and activators of transcription in cells exposed to polypeptide growth factors. Although initially characterized for their role in activating interferon-responsive genes, they have been subsequently shown to be activated in response to many cytokines and growth factors, including TGF-α (43, 44). We previously reported that constitutive activation of Stat3 is linked to both production of TGF-α and expression of EGFR in SCCHN cells *in vitro* (26). In this study, we extend these observations to an *in vivo* model of head and neck cancer and demonstrate that constitutive Stat3 activation is associated with EGFR autocrine stimulation of human squamous cell carcinomas.

Increasing evidence supports the critical role of Stat3 in transformation and tumor progression. Constitutive Stat3 activation has been described in cells transformed by diverse oncoproteins (18). Stat3 activation is essential for transformation of fibroblasts induced by v-Src in which Src kinase induced Stat3-mediated gene regulation (21). In these studies, dominant-negative Stat3 suppressed Src-mediated transformation but had no effect on ras-induced transformation (20, 21). Experiments demonstrating that constitutively activated Stat3 drives transcription and transforms cells independently of a tyrosine kinase oncogene were recently reported (45). Our finding of increased Stat3 in the histologically normal mucosa from patients with head and neck cancer suggests that activation of this oncogene may be an early event in squamous epithelial carcinogenesis.

The downstream events from constitutively active Stat3 are incompletely understood. Tumor progression could be facilitated by activation of genes that stimulate proliferation and/or block apoptosis. Cyclin D1 mRNA is reportedly increased in cells transformed by Stat3 because of activated gene transcription (45). Stat3 appears to serve an anti-apoptotic function in both normal and transformed cells. Deletion of Stat3 results in very early embryonic lethality, possible because of apoptosis of critical myeloid precursors (46). T-cell proliferation is facilitated by Stat3 activation, which prevents apoptosis independently of Bcl-2 (37). Abrogation of Stat3 has been shown to induce apoptosis in a murine melanoma model (47). Evidence is accumulating to suggest that Stat3 mediation of apoptosis inhibition may be caused by regulation of apoptotic regulatory proteins. Stat3 regulates transcription from the bcl-x promoter (25), and cells transformed by constitutively active Stat3 have elevated levels of Bcl-x_L mRNA (45). Our findings of increased tumor apoptosis associated with decreased Bcl-x_L protein expression after intratumoral injection of a Stat3 antisense expression construct support an interaction between Stat3 and bcl-x gene expression that regulates apoptosis.

Although several potential EGFR signaling pathways have been described, strategies that interfere with individual signaling molecules have not resulted in inhibition of cell growth. Because of its intrinsic tyrosine kinase activity, EGF receptors can directly induce STAT phosphorylation. Transformed squamous epithelial cells overexpress EGFR and its ligand, TGF-α, which results in autocrine growth *in vitro* and *in vivo* (5, 10, 30, 48). We previously reported that Stat3 is constitutively activated in SCCHN cells *in vitro* as a result of TGF-α/EGFR autocrine stimulation and that targeting Stat3, by using several strategies, reduced proliferation of SCCHN cells (26). The detection of increased Stat3 in SCCHN tumors that is abrogated by EGFR antisense gene therapy suggests that Stat3 may be a critical component of EGFR autocrine signaling *in vivo* and may serve as a therapeutic target. Our finding of elevated Stat3 expression/activation levels in normal mucosa, which is at high risk for cancer formation, further pinpoints Stat3 activation before phenotypic transformation. The development of strategies that target Stat3 could therefore improve efforts to prevent this malignancy.

This work was supported in part by The Eye and Ear Foundation, The Veterans' Affairs Hospitals Research Foundation, and National Institutes of Health Grants CA01760, CA72526, and CA77308 (to JRG).

1. Slaughter, D. P., Southwick, H. W. & Smejkal W. (1953) *Cancer* **6,** 963–968.
2. Jones, A. S., Morar, P., Phillips, D. E., Field, J. K., Husband, D. & Helliwell, T. R. (1995) *Cancer* **75,** 1343–1353.
3. Larson, J. T., Adams, G. L. & Fattah, H. A. (1990) *Otolaryngol. Head Neck Surg.* **103,** 14–24.
4. Rubin Grandis, J. & Tweardy, D. J. (1993) *Cancer Res.* **53,** 3579–3584.
5. Rubin Grandis, J., Melhem, M. F., Barnes, E. L.& Tweardy D. J. (1996) *Cancer* **78,** 1284–1292.
6. Rubin Grandis, J., Tweardy, D. J. & Melhem M. (1998) *Clin. Cancer Res.* **4,** 13–20.
7. Rubin Grandis, J., Zeng, Q. & Tweardy D. J. (1996) *Nat. Med.* **2,** 237–240.
8. Moroni, M. C., Willingham, M. C. & Beguinot L. (1992) *J. Biol. Chem.* **267,** 2714–2722.
9. Nicolini, G., Miloso, M., Moroni, M. C., Beguinot, L. & Scotto L. (1996) *J. Biol. Chem.* **271,** 30290–30296.
10. Rubin Grandis, J., Chakraborty, A., Zing, Q., Melhem, M. F. & Tweardy D. J. (1998) *J. Cell. Biochem.* **69,** 55–62.
11. Coffer, P. J. & Kruijer, W. (1995) *Biochem. Biophys. Res. Commun.* **210,** 74–81.
12. Akira, S., Nishio, Y., Inoue, M., Wang, X. J., Wei, S., Matsusaka, T., Yoshida, K., Sudo, T., Naruto, M. & Kishimoto, T. (1994) *Cell* **77,** 63–71.
13. Zhong, Z., Wen, Z. & Darnell, J. E. (1994) *Science* **264,** 95–98.
14. Darnell, J. E., Kerr, I. M. & Stark, G. R. (1994) *Science* **264,** 1415–1421.
15. Ihle, J. N. (1996) *Cell* **84,** 331–334.
16. Darnell, J. E., Jr. (1998) *J. Interferon Cytokine Res.* **18,** 549–554.
17. Darnell, J. E. (1997) *Science* **277,** 1630–1635.
18. Garcia, R. & Jove, R. (1998) *J. Biomed. Sci.* **5,** 79–85.
19. Yu, C. L., Meyer, D. J., Campbell, G. S., Larner, A. C., Carter-Su, C., Schwartz, J. & Jove, R. (1995) *Science* **269,** 81–83.
20. Bromberg, J. F., Horvath, C. M., Besser, D., Lathem, W. W. & Darnell, J. E., Jr. (1998) *Mol. Cell. Biol.* **18,** 2553–2558.
21. Turkson, J., Bowman, T., Garcia, R., Caldenhoven, E., De Groot, R. P. & Jove, R. (1998) *Mol. Cell. Biol*. **18,** 2545–2552.
22. Watson, C. J. & Miller, W. R. (1995) *Cancer* **71,** 840–844.
23. Garcia, R., Yu, C. L., Hudnall, A., Catlett, R., Nelson, K. L., Smithgall, T., Fujita, D. J., Ethier, S. P. & Jove, R. (1997) *Cell Growth Differ.* **8,** 1267–1276.
24. Sartor, C. I., Dziubinski, M. L., Yu, C. L., Jove, R. & Ethier, S. P. (1997) *Cancer Res.* **57,** 978–987.
25. Catlett-Falcone, R., Landowski, T. H., Oshiro, M. M., Turkson, J., Levitzki, A., Savino, R., Ciliberto, G., Moscinski, L., Fernandez-Luna, J. L., Nunez, G., *et al.* (1999) *Immunity* **10,** 105–115.
26. Rubin Grandis, J., Drenning, S. D., Chakraborty, A., Zhou, M. Y., Zeng, Q., Pitt, A. S. & Tweardy, D. J. (1998) *J. Clin. Invest.* **102,** 1385–1392.
27. Sadowski, H. B., Shuai, K., Darnell, J. E., Jr. & Gilman, M. Z. (1993) *Science* **261,** 1739–1744.
28. Wong, P., Severns, C. W., Guyer, N. B. & Wrights, T. M. (1994) *Mol. Cell. Biol.* **14,** 914–922.
29. Wagner, B. J., Hayes, T. E., Hoban, C. J. & Cochran, B. H. (1990) *EMBO J.* **9,** 4477–4484.
30. He, Y., Zeng, Q., Drenning, S. D., Melhem, M. F., Tweardy, D. J., Huang, L. & Grandis, J. R. (1998) *J. Natl. Cancer Inst.* **90,** 1080–1087.
31. Sacks, P. G., Parnes, P. M., Gallick, G. E., Mansouri, Z., Lichtner, R., Satya-Prakash, K. L., Pathak, S. & Parsons, D. F. (1988) *Cancer Res.* **48,** 2858–2866.
32. Schwartz, L. H., Ozsahin, M., Zhang, G. N., Touboul, E., De Vataire, F., Andolenko, P., Lacau-Saint-Guily, J., Laugier, A. & Schlienger, M. (1994) *Cancer* **74,** 1933–1938.
33. Hierholzer, C., Kalff, J. C., Omert, L., Tsukada, K., Loeffert, J. E., Watkins, S. C., Billiar, T. R. & Tweardy, D. J. (1998) *Am. J. Physiol.* **275,** L611–L621.
34. Fukada, T., Hibi, M., Yamanaka, Y., Takahashi-Tezuka, M., Fujitani, Y., Yamaguchi, T., Nakajima, K. & Hirano, T. (1996) *Immunity* **5,** 449–460.
35. Weber-Nordt, R. M., Mertelsmann, R. & Finke, J. (1998) *Leuk. Lymphoma* **28,** 459–467.
36. Kaplan, D. H., Shankaran, V., Dighe, A. S., Stockert, E., Aguet, M., Old, L. J. & Schreiber, R. D. (1998) *Proc. Natl. Acad. Sci. USA* **95,** 7556–7561.
37. Takeda, K., Kaisho, T., Yoshida, N., Takeda, J., Kishimoto, T. & Akira S. (1998) *J. Immunol.* **161,** 4652–4660.
38. Takeda, K., Clausen, B. E., Kaisho, T., Tsujimura, T., Terada, N., Forster, I. & Akira, S. (1999) *Immunity* **10,** 39–49.
39. Rubin Grandis, J., Melhem, M. F., Gooding, W. E., Day, R., Holst, V. A., Wagener, M. M., Drenning, S. D. & Tweardy, D. J. (1998) *J. Natl. Cancer Inst.* **90,** 824–832.
40. Ulrich, A. & Schlessinger, J. (1990) *Cell* **61,** 203–212.
41. Hernandez-Sotomayor, S. M. & Carpenter, G. (1992) *J. Membr. Biol.* **128,** 81–89.
42. Kumar, V., Bustin, S. A. & McKay, I. A. (1998) *Cell Biol. Int.* **19,** 373–388.
43. Schindler, C. & Darnell, J. E., Jr. (1995) *Annu. Rev. Biochem.* **64,** 621–625.
44. Ihle, J. N. & Kerr I. M. (1995) *Trends Genet.* **11,** 69–74.
45. Bromberg, J. F., Wrzeszczynska, M. H., Zhao, Y., Pestrell, R. G., Albanese, C. & Darnell, J. E. (1999) *Cell* **98,** 395–303.
46. Takeda, K., Noguchi, K., Shi, W., Tanaka, T., Matsumoto, M., Yoshida, N., Kishimoto, T. & Akira, S. (1997) *Proc. Natl. Acad. Sci. USA* **94,** 3801–3804.
47. Niu, G., Heller, R., Catlett-Falcone, R., Coppola, D., Jaroszeski, M., Dalton, W., Jove, R. & Yu, H. (1999) *Cancer Res.* **59,** 5059–5063.
48. Rubin Grandis, J., Chakraborty, A., Melhem, M. F., Zeng, Q. & Tweardy, D. J. (1997) *Oncogene* **15,** 409–416.